Available online at www.sciencedirect.com

ScienceDirect

Energy Procedia 101 (2016) 488 – 495

Energy Procedia

71st Conference of the Italian Thermal Machines Engineering Association, ATI2016, 14-16 September 2016, Turin, Italy

Critical Analysis Of Dynamic Stall Models In Low-Order Simulation Models For Vertical-Axis Wind Turbines

Alessandro Bianchini[a], Francesco Balduzzi[a], Giovanni Ferrara[a], Lorenzo Ferrari[b]*

[a]*Dept. of Industrial Engineering, Università degli Studi di Firenze, via di Santa Marta 3, Firenze 50139, Italy*
[b]*CNR-ICCOM, Consiglio Nazionale delle Ricerche, via Madonna del Piano 10, Sesto Fiorentino 50019 Italy*

Abstract

The efficiency of vertical-axis wind turbines (VAWTs) still lacks from those of horizontal-axis rotors (HAWTs). To improve on efficiency, more accurate and robust aerodynamic simulation tools are needed for VAWTs, for which low-order methods have not reached yet a maturity comparable to that of HAWTs' applications. In the present study, the VARDAR research code, based on the BEM theory, is used to critically compare the predictiveness of some dynamic stall models for Darrieus wind turbines. Dynamic stall, connected to the continuous variation of the angle of attack on the airfoils, has indeed a major impact on the performance of Darrieus rotors. Predicted lift and drag coefficients of the airfoils in motion are reconstructed with the different dynamic stall models and compared to unsteady CFD simulations, previously validated by means of experimental data. The results show that low-order models are unfortunately not able to capture all the complex phenomena taking place during a VAWT functioning. It is however shown that the selection of the adequate dynamic stall model can definitely lead to a much better modelling of the real airfoils' behavior and then notably enhance the predictiveness of low-order simulation methods.

Peer-review under responsibility of the Scientific Committee of ATI 2016.

Keywords: Darrieus; wind turbine; dynamic stall; BEM; CFD; airfoil

1. Introduction

Increasing interest is presently being paid by researchers and industrial manufacturers in re-discovering vertical axis wind turbines (VAWTs), after most major research projects came to a standstill in the mid 90's [1]. The inherent

* Corresponding author. Tel.: +39-055-275-8797; fax: +39-055-275-8755.
E-mail address: lorenzo.ferrari@iccom.cnr.it

Peer-review under responsibility of the Scientific Committee of ATI 2016.
doi:10.1016/j.egypro.2016.11.062

advantages of the VAWT (Darrieus) concept (i.e. independence on wind direction, generator positioned on the ground, low noise emissions, good performance in misaligned flows [2]) may outweigh their disadvantages in some specific application, e.g. the urban context [3]. At the present state-of-the-art, however, the global efficiencies of Darrieus turbines still lack from those of horizontal axis rotors (HAWTs) [1], due to their intrinsically more complex aerodynamics coming from the revolution of the blades around an axis orthogonal to flow direction. This generates a continuous variation of the angle of attack, which leads to additional phenomena, like for example dynamic stall [4].

Several semi-empirical methods and correlations have been proposed to account for VAWT's dynamic stall in low-order simulation models (e.g. the Blade Element Momentum Theory - BEM), mainly adapting the original ones developed for helicopter blades [1]. Even though more accurate tools are today available for the simulation [5], low-order methods still represent an industry standard, especially in the preliminary design phase. On this basis, the enhancement of their predictiveness can still provide notable benefits to a more effective design and development of VAWTs [6]. In the present study, the VARDAR research code is then used to critically compare the predictiveness of some widely used dynamic stall models for Darrieus wind turbines by comparing the corrected polars to those obtained upon analysis of calibrated CFD simulations.

Nomenclature

a	induction factor	[-]
A_M	empirical constant of the Berg model	[-]
c	blade chord	[m]
c_L, c_D, c_P	lift, drag, power coefficients	[-]
F_n, F_t (C_n, C_t)	normal, tangential forces (force coefficients)	[N]
R, D, H	turbine radius, diameter, height	[m]
T	torque	[Nm]
TSR	tip-speed ratio	[-]
U	wind speed	[m/s]
W	relative speed on the airfoil	[m/s]
α	incidence angle (AoA)	[deg]
β	pitch angle	[deg]
ϑ	azimuthal angle	[deg]
ρ	air density	[kg/Nm^3]
ω	revolution speed	[rad/s]

2. Simulation codes and case study

2.1. The VARDAR code

The VARDAR research code has been developed by the Department of Industrial Engineering of the Università degli Studi di Firenze, Italy. The code makes use of the BEM theory, by which the rotor performance is calculated coupling the momentum equation in the mainstream direction of the wind and a lumped-parameters aerodynamic analysis of the interactions between the airfoils in motion and the oncoming flow by means of pre-calculated polars (e.g. [1]). In particular, the VARDAR code has been specifically developed for H-Darrieus wind turbines based on the Double Multiple Streamtubes Approach with Variable Interference Factors (DMSV), originally proposed by Paraschivoiu [1] (Fig. 1a), which was the further developed with specific sub-models.

In this approach, the elementary torque for each azimuthal position is therefore given by Eq. 1:

$$T_{blade}(\vartheta) = F_t \cdot R = \frac{1}{2}\rho c W_\vartheta{}^2 C_{t(\vartheta)} RH \tag{1}$$

$$C_t = C_L \cdot \sin\alpha - C_D \cdot \cos\alpha \tag{2}$$

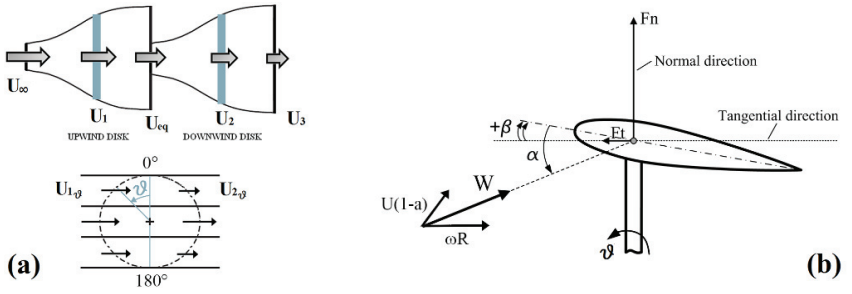

Fig. 1. (a) DMSV modeling; (b) convention for angles and forces on the airfoil.

where C_t (Eq. 2) is the tangential force coefficient in the reference system of the rotating blade (Fig. 1b). W represents the relative velocity in the upwind or downwind half, respectively, given by the vector sum of peripheral speed and wind speed (properly reduced by the induction factors). The modulus of W is given by Eqs. 3 and 4:

$$\left|W_{up}\right| = \sqrt{\left[(1-a)\cdot U_\infty \cdot \sin(\vartheta-\beta)\right]^2 + \left[(1-a)\cdot U_\infty \cos(\vartheta-\beta)+\omega R\right]^2} \quad (3)$$

$$\left|W_{down}\right| = \sqrt{\left[(1-a_2)\cdot U_{eq} \cdot \sin(\vartheta-\beta)\right]^2 + \left[(1-a_2)\cdot U_{eq} \cos(\vartheta-\beta)+\omega R\right]^2} \quad (4)$$

The value U_{eq} in Eq. 4 represents the wind velocity between the two actuator disks (see Fig. 1a). The Glauert's correction for the BEM theory is taken into account [7], together with the corrections due to blades finite Aspect Ratio, using the Lanchester-Prandtl model [8]. As will be discussed later on in the study, several dynamic stall models are available in the VARDAR code, as well as a specific module to account for the streamtubes' expansion along the flow path. For additional details on the code please refer to [9-12]. The prediction capabilities of the VARDAR code have been validated during a several-years' experience in the design of three real H-Darrieus rotors, having swept areas of 1.0, 2.5 and 5.0 m^2, respectively, and two or three blades, either straight or helix-shaped. The 1:1 models of all the rotors (two made of reinforced plastic and one of painted aluminum alloy) were tested in large wind tunnels (both with closed and open-jet). In all cases, the code was able to correctly predict both the power curves at different wind speeds and the starting ramps of rotor and is then considered fully predictive for the turbine type investigated in this study. For further details on the code validation please refer to [10-11].

2.2. Dynamic stall models

In the present study, three dynamic stall models were compared, selected among the most used ones in BEM simulations of Darrieus VAWTs [1]. For brevity reasons, no information about their numeric implementation can be provided here. Full details can be found, however, in [1]. The models are:

- **Strickland model** - The model [13] was the first adaptation of the Gormont's theory from helicopter blades to VAWTs. The hysteresis response of an airfoil is empirically mimicked by defining a reference angle of attack at which the static 2D aerodynamic coefficients of the airfoil are considered. The flow is considered incompressible and expressions were specialized for symmetric airfoils.
- **Paraschivoiu model** - Since it was proven experimentally that a high-level turbulence delays the onset of dynamic stall, Paraschivoiu et al. [1] proposed to apply the Strickland model only in regions of low turbulence, i.e. only in azimuthal positions between -90° and +90° in Fig. 1(a).
- **Massè and Berg model** - The model modifies the computation of dynamic coefficients based on a linear interpolation between the dynamic ones calculated with the Gormont's model and the static coefficients [14]. The empirical constant A_M is also added.

It has to be noted that other models are presently available for similar analyses, e.g. the *ONERA* model [15] or the Beddoes-Leishman model in indicial formulation [16]. In particular, the latter one has been recently analyzed by the authors [6] when applied to the Lifting Line Theory, revealing a good accuracy and a sound agreement with the Berg model. For these reasons, it will be included in the VARDAR code in the near future.

2.3. Case study

A case study for the analyses was first selected based on a previous work [17], i.e. a single-bladed rotor using a NACA 0018 airfoil with a chord-to-radius ratio (*c/R*) of 0.114. By doing so, the interaction between different blades was not accounted for since it was thought not to be part of the main focus of the analysis, which was instead focused on the evaluation of dynamic stall models. The airfoil has a chord c=0.2 m and rotates in a Darrieus-like path (null pitch angle β – Fig. 1(b) - with respect to the tangential direction) having a radius R=1.75 m under a wind speed U=8 m/s. Additional model's details can be found in [17].

2.4. CFD simulations

Due to the extreme complexity of obtaining reliable experimental data of the flow field around an airfoil in Darrieus-like motion, CFD simulations were carried out to mimic the airfoil's behaviour.

The commercial code ANSYS® FLUENT® [18] was used in a two-dimensional form to solve the time-dependent unsteady Reynolds-Averaged Navier-Stokes equations. The fluid was air, modeled as an ideal compressible gas with standard ambient conditions, i.e. a pressure of 1.1×10^5 Pa and a temperature of 300 K. The authors have presented in recent works [19-20] the assessment and validation of the main settings that have been applied to the CFD simulations, which have also been validated against experimental data obtaining good agreement [17]. The main simulation settings are reported in Tab. 1; for additional details see [17,19,20]. Fig. 2 reports the calculated power coefficient curve of the airfoil.

Tab. 1. Main features of the CFD test case.

Operating Conditions	
Wind Speed (U)	8.0 [m/s]
TSR	1.0 - 4.7
Main CFD parameters	
Turbulence Model	*κ-ω SST*
Algorithm	Transient - Coupled
y^+ on the airfoil	<1
Timestep size	function of TSR [16] → 0.135÷0.5 deg
Mesh type	Hybrid: B.L. with quads-triangles outside
Mesh Size [# elements]	~ 400000

Fig. 2. CFD results: c_P vs. *TSR*.

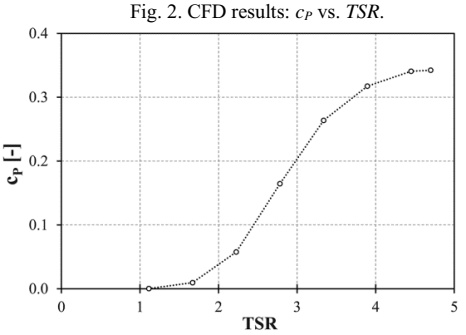

3. Data processing

In a previous study [6], the authors showed that, by using a proper dynamic stall model, a good accuracy of low-order simulation codes can be achieved, both in terms of power coefficient curve and of torque profile over the revolution. This is, however, true for medium-high TSRs, where the incidence variations are contained and the flow is mainly attached to the blades. In case of lower TSRs, where large separations occur, the accuracy of these codes becomes lower, especially in the prediction of the torque profile at a given TSR, since they are not able to properly predict the effects of vortices and separated flows.

To assess the accuracy of dynamic stall models, in particular, focus was here put on the comparative analysis of the lift and drag coefficients that are used in BEM simulations. In particular, the aerodynamic polars corrected by means of the dynamic stall models in the VARDAR code were compared to those reconstructed from the computed CFD flow field. These latter ones were estimated by reversing Eqs. (1) and (2), in which the blade torque was directly obtained from CFD. In doing so, the incidence angle was unfortunately not available from simulations and very hardly predictable, especially for all azimuthal positions with stalled flow [17]. To overcome this criticality, the incidence angle was directly borrowed from BEM simulations [5]. As a result, data reconstructed from CFD (referred to as "Virtual CFD" in the rest of the analysis) are suggestive of the aerodynamic coefficients that should be applied to a BEM code to match the CFD data (even if additional inner iterations on the induction factor would be needed in order to be fully coherent). Moreover, polars including dynamic stall modeling were also compared to the static coefficients, taken from a recent study [17] and reported for the average Reynolds number attended during

the revolution at the relevant TSR. Please note that, according to recent studies on virtual camber [17], the performance of the symmetric NACA 0018 in cycloidal motion must be compared to that of a virtually cambered airfoil (outward concavity) in straight flow with the camber line defined by its arc of rotation.

4. Results and discussion

Three TSRs were selected to analyze the results (TSR=2.2, 3.3 and 4.4), corresponding to three, strongly different, attended functioning conditions. At the lower TSR, large separations are in fact expected, progressively reducing by increasing the revolution speed up to the higher TSR, where the incidence angle variation is thought to become small enough to reduce the impact of stalled azimuthal positions during the revolution. Figures 3, 4 and 5 report the reconstructed lift and drag coefficients at TSR=2.2, TSR=3.3 and TSR=4.4, respectively.

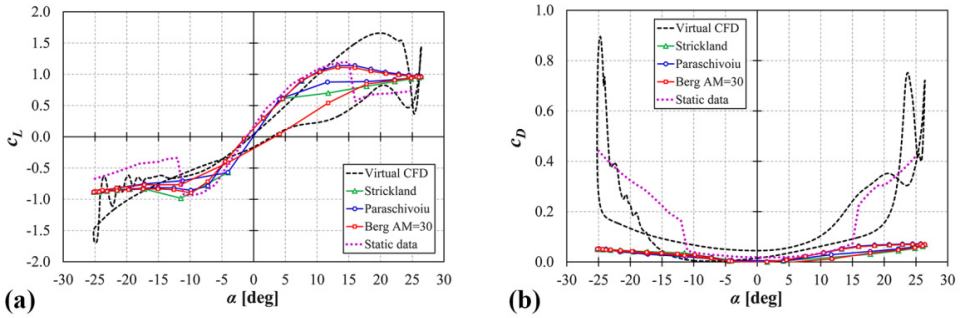

Fig. 3. (a) Lift coefficients @ TSR=2.2; (b) Drag coefficients @ TSR=2.2.

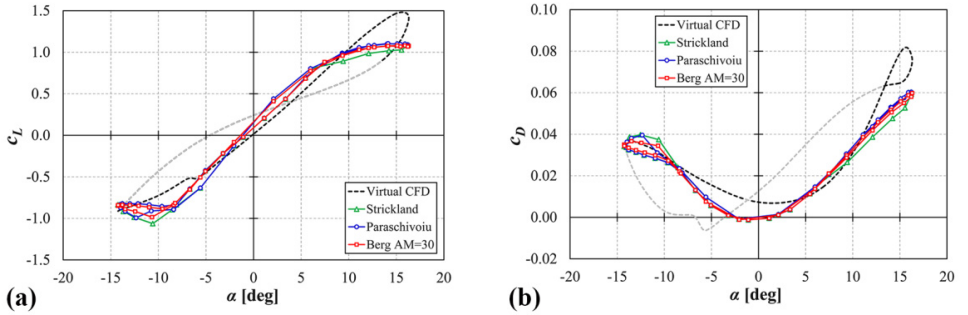

Fig. 4. (a) Lift coefficients @ TSR=3.3; (b) Drag coefficients @ TSR=3.3.

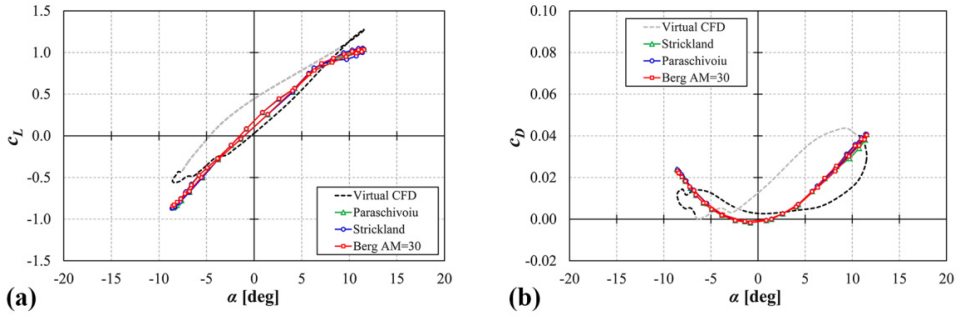

Fig. 5. (a) Lift coefficients @ TSR=4.4; (b) Drag coefficients @ TSR=4.4.

In Fig. 3, the static polars of the airfoil at a reference Reynolds number of 150000 are also reported; these data indeed correspond to those tabulated within the BEM code that would be used in case no dynamic stall model is enabled in the simulations. Upon examination of the figure, it is apparent that the real aerodynamic behaviour of the airfoil in motion is notably different from its attended static coefficients. All the considered stall models positively modified the polars (especially the lift one) by introducing the hysteresis cycle at high AoAs. Above all, the Berg model with A_M = 30 [6] ensured the best accuracy, with a better estimation of the cycle amplitude for positive AoAs. According to [17], the maximum lift was overestimated by CFD and the drag prediction was generally poorer. In particular, it is worth remarking that the application of the dynamic stall models implied the lack of the marked increase of drag in correspondence with the abrupt lift drop at the static stall angle. It is also worth highlighting that a low-order model like the BEM one was anyhow not able to mimic higher-order aerodynamic phenomena, like macro vortices detaching from the blades, whose effects are clearly visible in the polars near α=25° and in the region between α=-10° and α=-25°. For example, Fig. 6 reports the vorticity contours calculated by CFD in correspondence to two relevant points in the lift polar, labelled as (a) and (b).

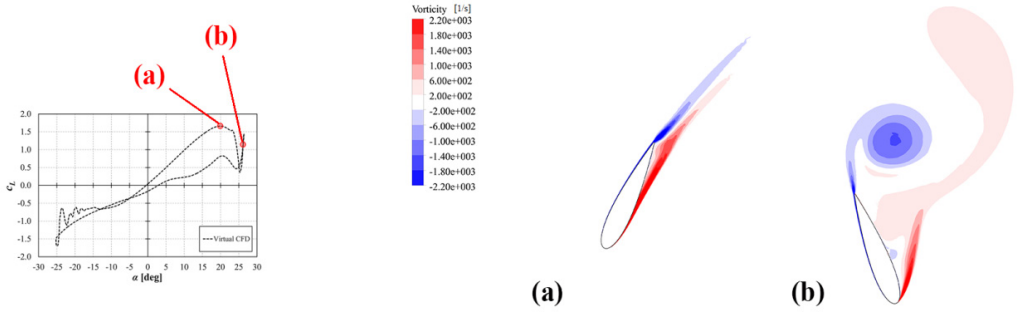

Fig. 6. Vorticity contours over the airfoil @ TSR=2.2: (a) ϑ=65° (α=20°); (b) ϑ=110° (α=25°).

From a perusal of the contours, it is apparent that in (a) the flow is mostly attached to the blade; the aerodynamic performance can be then described with the conventional lumped parameter analysis based on lift and drag coefficient. Conversely, at ϑ=110° the airfoil experiments a deep-stall conditions, the flow being almost completely separated and large vortices detaching alternatively from the leading and trailing edges [11]. In these conditions, the use of the aerodynamic coefficients to describe the airfoil's performance is not effective (see the hypothetical lift polar of Fig. 3(a)) since the vortices induce pulsations in the aerodynamic forces exerted by the airfoil itself.

Figures 4 and 5 instead report the lift and drag coefficients at higher TSRs. CFD-based curves are partially reported in grey color, in correspondence to those values in which an analysis of the computed flow field revealed that the AoA estimated with the BEM model was substantially different from the real flow on the airfoil. For example, Fig. 7 reports a snapshot of pressure contours at TSR=4.4 in the specular azimuthal positions of ϑ=0° and ϑ=180°. In these positions, the simplified analysis carried out by the BEM model would in fact predict a theoretically null incidence in both cases, since the vectors of the absolute wind speed and the peripheral speed are aligned on the same direction [1]. Upon examination of Fig. 7, however, if this assumption is generally true in case of ϑ=0° (where the pressure pattern is almost symmetrical in the pressure and suction sides of the airfoil), it is apparent that at ϑ=180° the airfoil experiments a non-null incidence, due to a distorted direction of the absolute wind speed. This represents a main limitation of a low-order method like the BEM analysis, since no correction model is presently available to account for flow distortions of the wind speed induced by the flow-turbine interaction [21]; bias errors are then unavoidably induced by the use of tabulated aerodynamic polars. If one analyzes the polars, it can be noticed that once again the maximum lift was slightly underestimated by the BEM model, while, in general, a satisfactory matching between CFD-based data and dynamic stall models was achieved, especially for increasing incidences. Even if the described mismatch of AoAs with CFD did not allow a direct comparison, the Berg model was again the one inducing the major modifications to the polars and somehow able to more closely reproduce the hysteresis cycle due to dynamic stall. The drag coefficient, slightly affected by the dynamic stall models, was constantly underestimated by CFD calculations with respect to the attended one based on static polars [17].

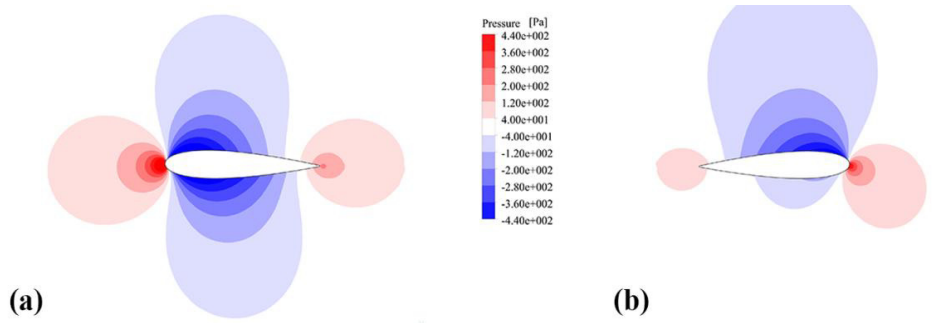

Fig. 7. Pressure pattern over the airfoil @ TSR=4.4: (a) ϑ=0° (theoretical α=0°); (b) ϑ=180° (theoretical α =0°).

For the sake of completeness, Tab. 2 reports the comparison between the power coefficient values predicted by CFD and those calculated with the VARDAR code. Again, it can be noticed that, in general, the Berg model ensured a better matching with CFD data, even if the major improvements have to be looked for in the description of the torque profile, as already discussed in [6].

Tab. 2. Comparison of power coefficient values.

	CFD	**BEM simulations**		
TSR		*Strickland*	*Paraschivoiu*	*Berg*
2.2	0.057	0.087	0.088	0.085
3.3	0.261	0.253	0.256	0.252
4.4	0.338	0.358	0.359	0.355

A final remark on the use of dynamic stall models in BEM simulations is the influence of the Reynolds number in the selection of lift and drag coefficient to be used during the calculation. To this purpose, in Fig. 8 the experimental lift polar at Re=150k is compared to that predicted at TSR=2.2 using either the original VARDAR code with the Berg model (A_M=30) (i.e. with an interpolation on tabulated polars at each azimuthal position as a function of incidence and Reynolds number) or a modified version using a data set for aerodynamic coefficients independent on the Reynolds number (fixed at Re=150k). Upon examination of the figure, one can readily notice that the interpolation on the Reynolds number has a major impact on the simulations using a BEM approach. In particular, the superior accuracy of the Berg model, already discussed in Fig. 3(a) is mostly based on the stronger sensitivity of this model to the inflow velocity on the airfoil (see [1,14]).

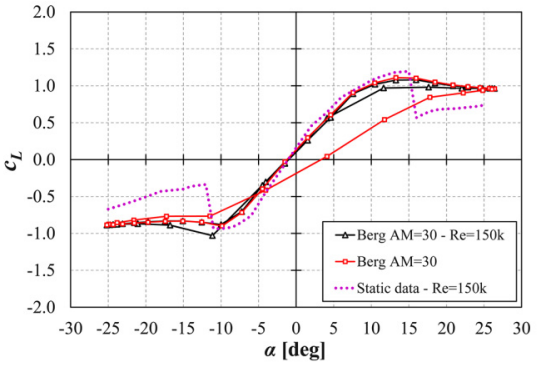

Fig. 8. Comparison between the static lift polar at Re=150k and those predicted by the BEM code with the Berg dynamic stall model at TSR=2.2 either with or without accounting for Reynolds number variation.

5. Conclusions

In this study, a critical analysis of three dynamic stall models for use in low-order simulations of Darrieus VAWTs was carried out. The analysis confirmed that the real behavior of airfoils in motion is much different in comparison to their attended aerodynamic performance based on 2D static polars. In particular, low-order models are not able to capture all the complex phenomena taking place during a VAWT functioning, like the effects of macro vortices detaching form the airfoils at high AoAs or the distortion of the oncoming wind speed.

Within this context, the use of a dynamic stall model in BEM codes is essential. Based on the present study (which is, anyhow, in line with the most recent literature), the use of the Berg model with a high value of A_M (≈ 30) ensured the best accuracy, especially at low TSRs, where dynamic stall effects are magnified. This was mainly due to the higher sensitivity of this model to the predicted Reynolds number of the relative flow on the airfoil.

Acknowledgements

Thanks are due to Prof. Ennio A. Carnevale of the *Università degli Studi di Firenze* for supporting this research activity. The authors would like also to acknowledge Dr. Domenico Fiorini for his contribution to the study.

References

[1] Paraschivoiu I. Wind Turbine Design with Emphasis on Darrieus Concept. Canada: Polytechnic International Press; 2002.
[2] Bianchini A, Ferrara G, Ferrari L, Magnani S. An improved model for the performance estimation of an H-Darrieus wind turbine in skewed flow. Wind Engineering 2012;36(6): 667-686.
[3] Balduzzi F, Bianchini A, Carnevale EA, Ferrari L, Magnani S. Feasibility analysis of a Darrieus vertical-axis wind turbine installation in the rooftop of a building. Applied Energy 2012; 97: 921–929.
[4] Simao-Ferreira C, van Zuijlen A, Bijl H, van Bussel G, van Kuik G. Simulating dynamic stall on a two-dimensional vertical-axis wind turbine: verification and validation with particle image velocimetry data. Wind Energy2010; 13:1-17.
[5] Allet A, Hallè S, Paraschivoiu I. Numerical Simulation of Dynamic Stall Around an Airfoil in Darrieus Motion. Journal of Solar Energy Engineering 1999;121:69-76.
[6] Marten D, Bianchini A, Pechlivanoglou G, Balduzzi F, Nayeri CN, Ferrara G, Paschereit CO, Ferrari L. Effects of airfoil's polar data in the stall region on the estimation of Darrieus wind turbines performance. Proc. of the ASME Turbo Expo 2016, Seoul, South Korea, June 13-17, 2016.
[7] Marshall L, Buhl Jr J. A New Empirical Relationship between Thrust Coefficient and Induction Factor for the Turbulent Windmill State. Report NREL/TP-500-36834, National Renewable Energy Laboratory, CO, USA, 2005.
[8] Abbott IH, Von Doenhoff AE. Theory of Wing Sections. New York, USA: Dover Publications Inc.; 1959.
[9] Bianchini A, Ferrari L, Magnani S. Start-up behavior of a three-bladed H-Darrieus VAWT: experimental and numerical analysis. Proceedings of the ASME Turbo Expo 2011, Vancouver (Canada), June 6-10, 2011.
[10] Bianchini A, Carnevale EA, Ferrari L. A model to account for the Virtual Camber Effect in the Performance Prediction of an H-Darrieus VAWT Using the Momentum Models. Wind Engineering 2011;35(4):465-17.
[11] Balduzzi F, Bianchini A, Maleci R, Ferrara G, Ferrari L. Blade design criteria to compensate the flow curvature effects in H-Darrieus wind turbines. Journal of Turbomachinery 2014;137(1):1-10.
[12] Bianchini A, Ferrara G, Ferrari L. Design guidelines for H-Darrieus wind turbines: Optimization of the annual energy yield. Energy Conversion and Management 2015;89:690-707.
[13] Strickland JH, Webster BT, Nguyen T. A vortex model of the Darrieus turbine: an analytical and experimental study. Sandia National Laboratories, Albuuqerque, N.M., tech. rep. SAND 79-7058, 1980.
[14] Massé B. Description de deux programmes d'ordinateur pour le calcul des performances et des charges aérodynamiques pour les éoliennes à axe vertical. tech. rep. IREQ-2379, 1981.
[15] McAlister KW, Lambert O, Petot D. Application of the ONERA model of dynamic stall. Technical Report NASA TR 84-A-3, National Aeronautics and Space Administration, 1984.
[16] Leishman JG, Beddoes, TS. A Generalized Model for Airfoil Unsteady Aerodynamic Behaviour and Dynamic Stall Using the Indical Method. Proc. of the 42nd Annual Forum of the American Helicopter Society, Washington D. C., USA, 1986.
[17] Rainbird J, Bianchini A, Balduzzi F, Peiro J, Graham JMR, Ferrara G, Ferrari L. On the Influence of Virtual Camber Effect on Airfoil Polars for Use in Simulations of Darrieus Wind Turbines. Energy Conversion and Management 2015;106:373-384.
[18] ANSYS®, Inc., 2015, FLUENT® Theory Guide, release 16.0.
[19] Balduzzi F, Bianchini A, Ferrara G, Ferrari L. Dimensionless numbers for the assessment of mesh and timestep requirements in CFD simulations of Darrieus wind turbines. Energy 2016;97(15 February 2016):246-261.
[20] Balduzzi F, Bianchini A, Maleci R, Ferrara G, Ferrari L. Critical issues in the CFD simulation of Darrieus wind turbines. Renewable Energy 2016;85(Jan 2016):419-435.
[21] Bianchini A, Balduzzi F, Ferrara G, Ferrari L. Virtual incidence effect on rotating airfoils in Darrieus wind turbines. Energy Conversion and Management 2016;111(1 March 2016):329-338.